



## AUTAPSE TURNS NEURON INTO OSCILLATOR

CHRISTOPH S. HERRMANN\* and ANDREAS KLAUS

*Max-Planck-Institute of Cognitive Neuroscience*

*Postfach 500 355, 04303 Leipzig, Germany*

*\*Magdeburg University, P.O. Box 4120, 39016 Magdeburg, Germany*

*\*herrmann@cns.mpg.de*

Received May 19, 2002; Revised November 1, 2002

Recently, neurobiologists have discovered axons on neurons which synapse on the same neuron's dendrites — so-called autapses. It is not yet clear what functional significance autapses offer for neural behavior. This is an ideal case for using a physical simulation to investigate how an autapse alters the firing of a neuron. We simulated a neural basket cell via the Hodgkin–Huxley equations and implemented an autapse which feeds back onto the soma of the neuron. The behavior of the cell was compared with and without autaptic feedback. Our artificial autapse neuron (AAN) displays oscillatory behavior which is not observed for the same model neuron without autapse. The neuron oscillates between two functional states: one where it fires at high frequency and another where firing is suppressed. This behavior is called “spike bursting” and represents a common pattern recorded from cerebral neurons.

*Keywords:* Autapse; Hodgkin–Huxley neuron.

### 1. Introduction

In the past couple of years, neurobiologists have found that axons, which propagate the neuron's electrical activity to other neurons, sometimes feed back to the dendrites of the same neuron [Tamas *et al.*, 1997]. The term autapse has been coined for these auto-synapses (cf. Fig. 1). Autaptic connections had been known for some time, but had been considered as erroneous structures which only develop in cultured neurons. In a recent study, autapses have been found in 80% of the investigated neurons [Lübke *et al.*, 1996]. It is now assumed that they are a part of the neural architecture of the brain, but their functional role still remains unclear. It has been speculated that autapses might serve a self-inhibitory function [Bekkers & Stevens, 1991].

From a technical point of view, neurons with inhibitory autapses represent feedback oscillators. By demonstrating the functional behavior of such

autaptic neurons in a simulation, we wish to shed some light on possible mechanisms resulting from this type of feedback. A vast variety of experiments with animals and humans have shown that neural activity in the so-called gamma frequency range is seen in single-cell recordings [Gray *et al.*, 1989], the electroencephalogram (EEG) [Tallon-Baudry *et al.*, 1996] and magnetoencephalogram of the human brain [Tallon-Baudry *et al.*, 1997; Herrmann & Mecklinger, 2000]. The gamma frequency band ranges from about 20 to 80 Hz, but usually frequencies around 40 Hz are observed by authors in various brain regions [Başar-Eroglu *et al.*, 1996]. The question arises, why there are such stable frequencies of relatively long time periods in a dynamic system. Different mechanisms have been proposed to explain stable oscillatory behavior in neurons. Among them are models in which basal structures (e.g. the thalamus or basal ganglia)

---

\* Author for correspondence.

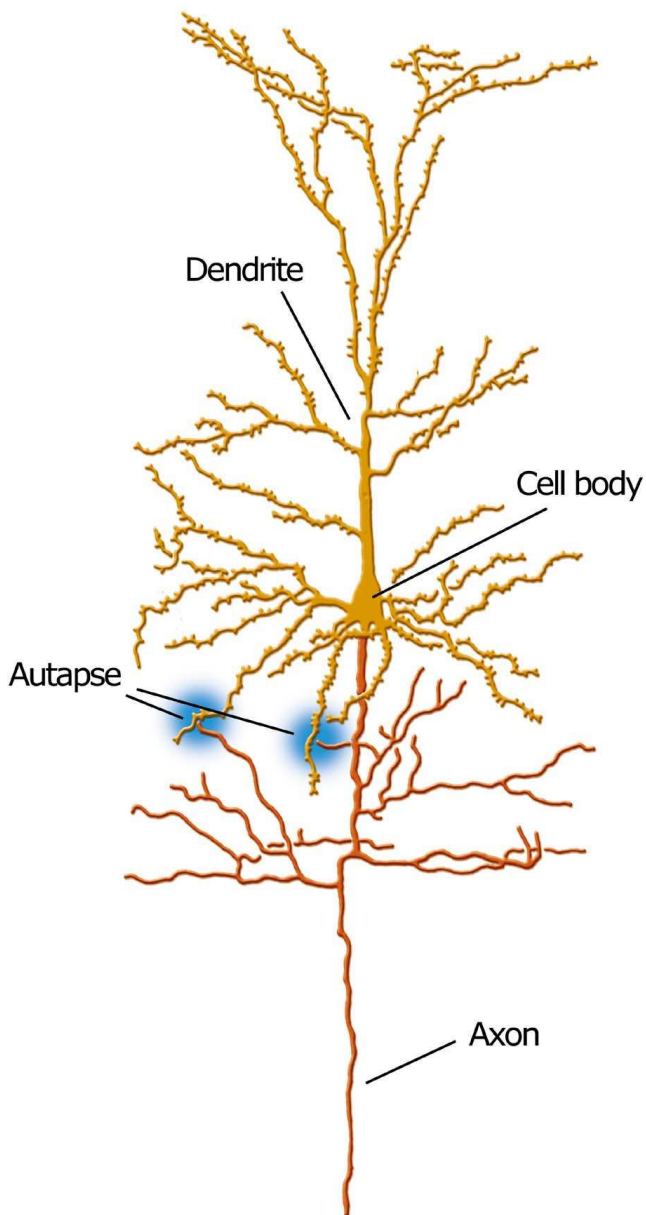


Fig. 1. Schematic drawing of an autapse. Dendrites and soma are in yellow, axon and autapse are in orange. Adapted from a drawing of a neuron without autapses from [Cajal, 1911].

synchronize other neurons [Zschocke, 1995], models which build up on dynamic system properties [Eckhorn *et al.*, 1990] and models in which single cortical neurons serve as gating neurons for adjacent neurons [Gray & McCormick, 1996]. Another possible explanation arises from the autaptic feedback. If each neuron represents a neural oscillator with autaptic feedback then it is very probable that the parameters of this autapse, like time delay and proximity to the soma, determine a resonance fre-

quency for the firing of the neuron. The neuron would then preferably oscillate at this frequency.

Here, we want to introduce an artificial neuron model with autaptic feedback and illustrate the possible relevance for neural computation in the brain.

## 2. Materials and Methods

In 1943, the idea to simulate neural activity by a simplified artificial neuron was introduced by McCulloch and Pitts [1943] but became only popular after the results of the Parallel Distributed Processing group [Rumelhart & McClelland, 1986]. Since then, the development of artificial neural networks has diverged into the two directions of *computationally simple* and *biologically plausible* architectures. The AAN which we want to introduce here falls into the class of biologically plausible neurons, since it models the anatomical components of biological neurons.

Figure 2 shows a schematical drawing of the components of a neuron. The biological neuron receives inputs over axons from other neurons via the dendrites of its dendritic tree. It sums up received input over time in its soma and generates output on its axon if a certain threshold is exceeded. This axon connects to other neurons where the process is repeated. In computationally simple neurons, this procedure is simulated by elements that sum up their weighted inputs. Each of  $i$  inputs  $in_i$  is at first multiplied by its weight term  $w_i$  and subsequently all weighted inputs are summed, leading to the net input  $net = \sum_i in_i \cdot w_i$ . The activation of the neuron then depends upon exceeding a threshold, i.e. the neuron is activated when its sum of weighted inputs exceeds a threshold. However, the true electrical behavior of a neuron is much more complicated.

To better understand neural computation, one has to move from this simplified artificial neuron to a more biologically plausible neuron. Let us briefly review the way a biological neuron works. A neuron is shielded from its outside (extracellular space) by a membrane. This membrane contains numerous channels which are selectively permeable for specific substances. The functionality of a neuron results mainly from these channels in its membrane, since they can vary the potential difference between intracellular and extracellular space (membrane potential). Let us sketch the excitation of one neuron over time: When a neuron is active it fires an action potential which then propagates along

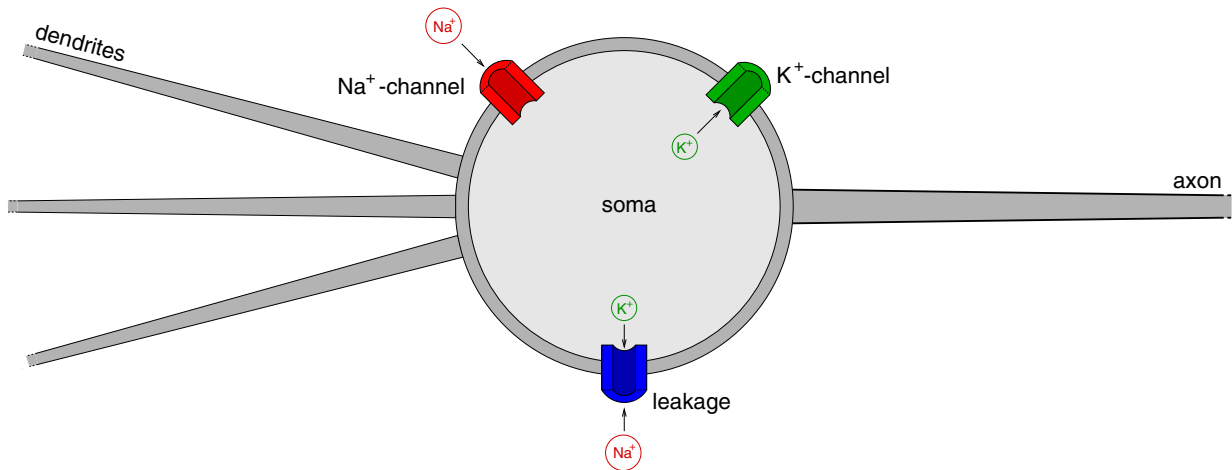


Fig. 2. Schematic diagram of a neuron with its basic components.

its axon to other neurons. At the end-points of an axon, synapses pour out so-called neurotransmitters. These neurotransmitters can open chemically sensitive ion channels inside the membrane of a neuron's dendrite. This is where information flow starts within a neuron. If a neurotransmitter opens a sodium channel ( $\text{Na}^+$ ), positively charged sodium particles can enter the dendrite. This moves the membrane potential of the neuron which is usually at a resting potential of about  $-70$  mV towards more positive values. If enough sodium channels are opened at many dendrites the potential of the neuron will reach a threshold. If this threshold is exceeded voltage-gated sodium channels in the soma will open, letting even more positively charged ions stream into the neuron (cf. red  $\text{Na}^+$  channel in Fig. 2). This leads to a so-called action potential — a sudden shift of the soma potential away from the negative resting-potential to a positive value. This action potential is then propagated along the axon to other neurons where the same process repeats. The action potential is eliminated after about 1 ms, because the sodium channels close shortly after opening and remain in a refractory state in which they cannot be reopened for about another ms. During this time, voltage-gated potassium channels (cf. green  $\text{K}^+$  channel in Fig. 2) let positively charged potassium ions ( $\text{K}^+$ ) flow out of the soma. This brings the soma potential back to the negative resting potential. A good overview of this topic is given by Rosenzweig *et al.* [2001] and a very thorough introduction to this topic is given by Kandel *et al.* [2000].

### 2.1. The Hodgkin–Huxley neuron

In order to account for this complex behavior, Hodgkin and Huxley [1952] developed a more realistic model-neuron which consists of electric equivalents of the ion channels inside the neuron's membrane. This model is shown as an electrical equivalent circuit in Fig. 3. It represents the sodium and potassium channels by resistors  $R_{\text{Na}}$  and  $R_{\text{K}}$ , respectively. The ion flow through these channels is represented by currents  $I_{\text{Na}}$  and  $I_{\text{K}}$  resulting from voltage sources  $E_{\text{Na}}$  and  $E_{\text{K}}$ , respectively. The membrane itself is represented by a capacitor  $C_m$ . An additional leakage current  $I_L$  represents ion channels which are neither selective for specific ions nor voltage-gated and thus lead to a constant leakage (cf. blue channel in Fig. 2). The membrane voltage,  $V_m$ , can be computed according to the formula for currents through a capacitor, since the current through the capacitor (membrane) is simply the sum of the inward and outward ion currents:

$$C_m \frac{dV_m}{dt} = I_{\text{Na}} - I_{\text{K}} + I_L \quad (1)$$

In the Hodgkin–Huxley model, changes of the membrane voltage are determined by the changes of the currents through the three types of channels. That is, when dendritic input shifts  $V_m$  above the threshold of the  $\text{Na}^+$  channels, a current  $I_{\text{Na}}$  will produce a voltage in  $R_{\text{Na}}$  making  $V_m$  more positive and thus representing the action potential. When  $V_m$  exceeds the threshold for  $\text{K}^+$  channels a current  $I_{\text{K}}$  will produce an inverse voltage in  $R_{\text{K}}$  and  $V_m$  will

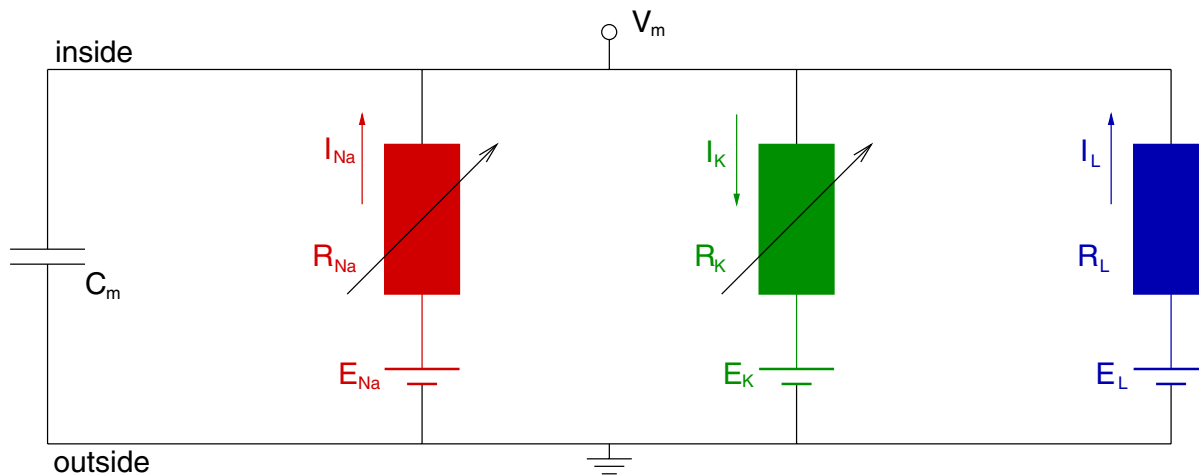


Fig. 3. Circuit diagram of a Hodgkin-Huxley neuron.

return to the resting potential. This model allows to obtain values of  $V_m$  as if recorded from a neuron but offers to investigate how changes in the neural architecture affect its behavior. Therefore, we chose to use this model to simulate autaptic feedback. For computation, we used the NEURON simulator by Hines and Carnevale [1995] which can be downloaded from [www.neuron.yale.edu](http://www.neuron.yale.edu). The simulator has been described in two recent journal articles [Hines & Carnevale, 1997, 2001].

## 2.2. The artificial autapse neuron

Many inhibitory neurons have been found to embody autapses, that feed back axonal action potentials to the own dendritic tree [Tamas *et al.*, 1997]. Therefore, we used an inhibitory neuron as a model for our artificial autapse neuron.

Only inhibitory feedback leads to stable behavior which may become oscillatory — positive feedback yields unstable behavior with the potential risk of saturation. The 40 Hz oscillations which might result from autaptic oscillations are often recorded from hippocampal neurons [Cobb *et al.*, 1995; Jefferys *et al.*, 1996]. Therefore, we chose to model a hippocampal neuron, since autapses have also been demonstrated within the hippocampus [Bekkers & Stevens, 1991]. The human hippocampus mainly consists of pyramidal neurons and basket cells [Gloor, 1998]. Pyramidal cells release excitatory neurotransmitter and are thus not suited for our model. Basket cells, however, serve as inhibitory inter-neurons and release the inhibitory neurotransmitter gamma-amino-butyric acid (GABA) [Kandel

*et al.*, 2000, p. 285]. Therefore, we modeled a hippocampal basket cell with an inhibitory GABA autapse (cf. Fig. 4). The exact parameters of our model cell are given in Sec. 5.

Inhibitory synapses like our autapse are frequently found close to the soma of a neuron [Kandel *et al.*, 2000, p. 22]. For this reason, our autapse feeds back to the soma of the basket cell rather than its dendrites where excitatory cells are usually located. Since we used a basket cell which make GABA<sub>A</sub> synapses [Gutnick, 1995, p. 90], the autapse is modeled via chloride channels ( $\text{Cl}^-$ ) which are typically opened by GABA [Kandel *et al.*, 2000, p. 217]. In order to include the autaptic inhibition into the current equation we introduced a current  $I_{\text{aut}}$  which is subtracted from the other ionic currents thus

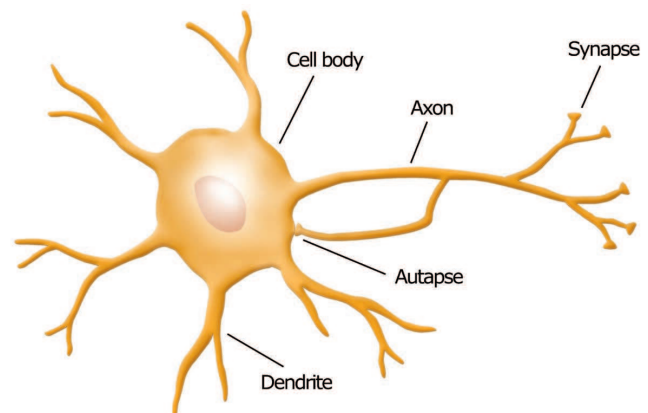


Fig. 4. Schematic drawing of a basket cell with autaptic feedback as used in our simulation.

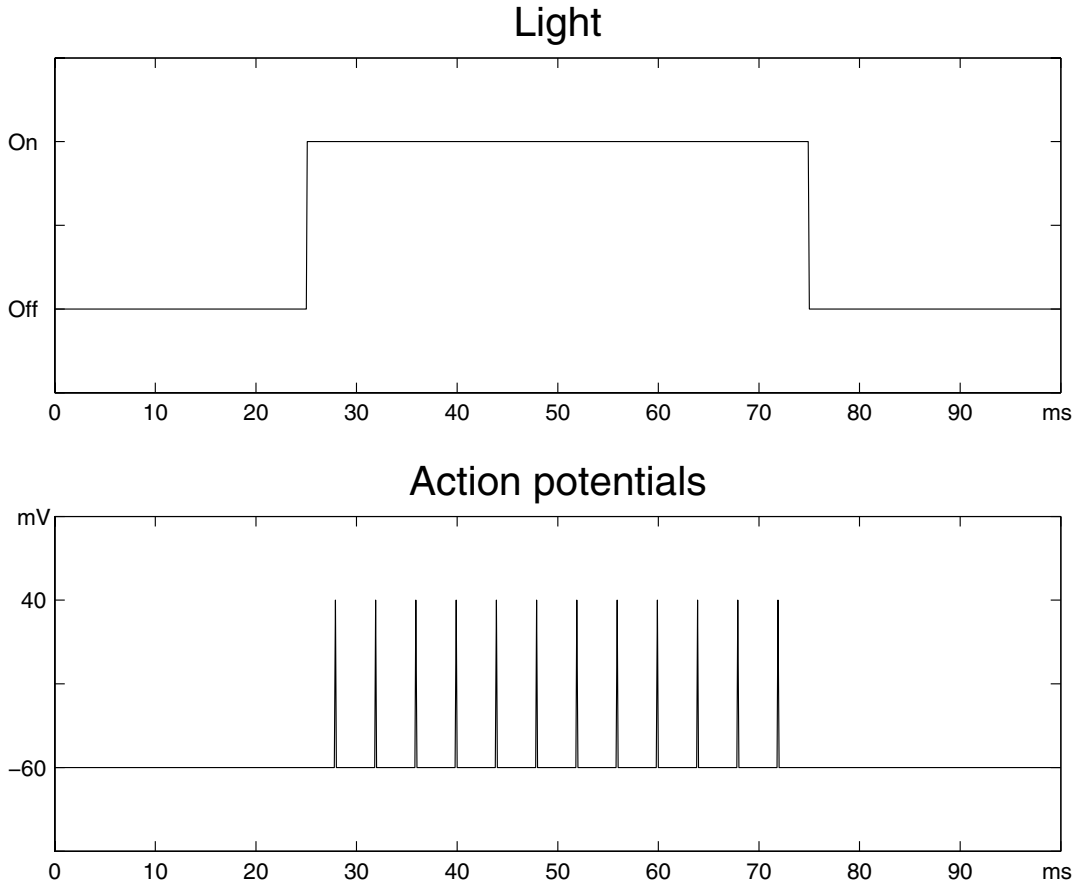


Fig. 5. Signal transduction: the light falling onto the retina is converted into action potentials which are propagated to visual cortex. Such a train of action potentials was used as dendritic input to our model neuron in order to simulate peripheral input.

diminishing the membrane potential. The conductivity of the channels is computed according to the following equation [Dayan & Abbott, 2001, p. 182].

$$G_{\text{aut}} = \varphi_{\text{aut}} G_{\text{aut-max}} (e^{-t/\tau_{\text{aut}1}} - e^{-t/\tau_{\text{aut}2}}) \quad (2)$$

where  $\varphi_{\text{aut}}$  is a normalization factor that assures that the peak of conductance is  $G_{\text{aut-max}}$  (parameters are given in Sec. 5).

Finally, we had to model the excitatory dendritic input to the neuron. As for the inhibitory autapse a further current was introduced into the model with opposite polarity which increases the membrane potential. This synaptic current was named  $I_{\text{syn}}$  leading to the following current balance equation:

$$C_m \frac{dV_m}{dt} = I_{\text{Na}} - I_{\text{K}} + I_L + I_{\text{syn}} - I_{\text{aut}} \quad (3)$$

The conductivity of the corresponding channels is computed according to the following equation (parameters are given in Sec. 5).

$$G_{\text{syn}} = \varphi_{\text{syn}} G_{\text{syn-max}} (e^{-t/\tau_{\text{syn}1}} - e^{-t/\tau_{\text{syn}2}}) \quad (4)$$

Fast spiking neurons are known to produce spike trains as high as 800 Hz and typically fire around 200 Hz [Gray & McCormick, 1996]. Therefore, the input to the dendrites was assumed to be a constant spike train of 200 Hz as it might be propagated from visual cortex to hippocampus due to visual stimulation (cf. Fig. 5).

### 3. Results

The main result of our work is the finding that the *artificial autapse neuron* (AAN) is capable of generating spike bursts comparable to those obtained in the biological neural system.

Figure 6 shows the axon potential of the AAN when excited with the input from Fig. 5. The input arrives at all five dendrites at the same time. Thus, the dendritic input at the soma exceeds the threshold and an action potential is generated. This action potential is propagated along the axon and feeds back into the soma via the autapse. The time-delay

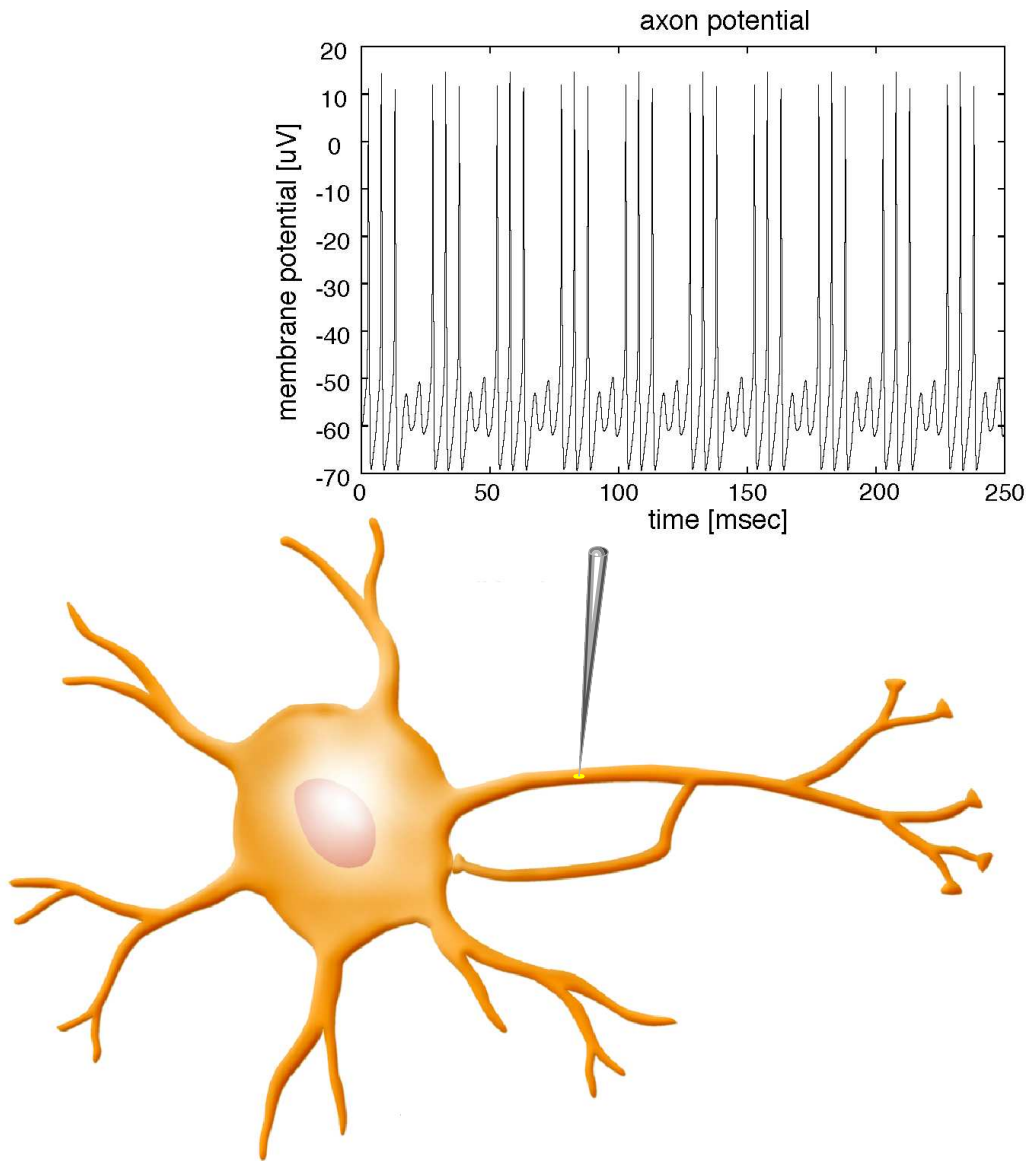


Fig. 6. Oscillatory activity of the artificial autapse neuron.

due to the finite propagation speed (approx 6 m/s) is negligible for the short autapse. However, the action potential is temporally smeared out due to the time constant of the autapse (4.2 ms). The first autaptic inhibitory postsynaptic potential (IPSP) does not affect the firing of the neuron, since it is too weak. After 3 autaptic IPSP have been summed up, the inhibition disables further dendritic input to reach the threshold (after about 20 ms). Then, no action potentials are generated for the next two input peaks, since the  $\text{Na}^+$  inflow at the dendrites does not exceed the  $\text{Cl}^-$  inflow at the soma. However, during this time also the inhibitory feedback

becomes weaker, since no action potentials are fed back via the autapse. Hence, after two missed action potentials, the autaptic feedback is too small to inhibit further dendritic input and the cycle starts from the beginning.

Figure 7 compares the behavior of the simulated basket cells with (right) and without (left) an autapse. The diagrams display the so-called phase plane which is commonly used to visualize the dynamic behavior of neurons [Haken, 1996; Freeman, 2000]. The conductivity of the potassium channels is displayed as a function of the membrane voltage. In case of no autaptic feedback (left) the

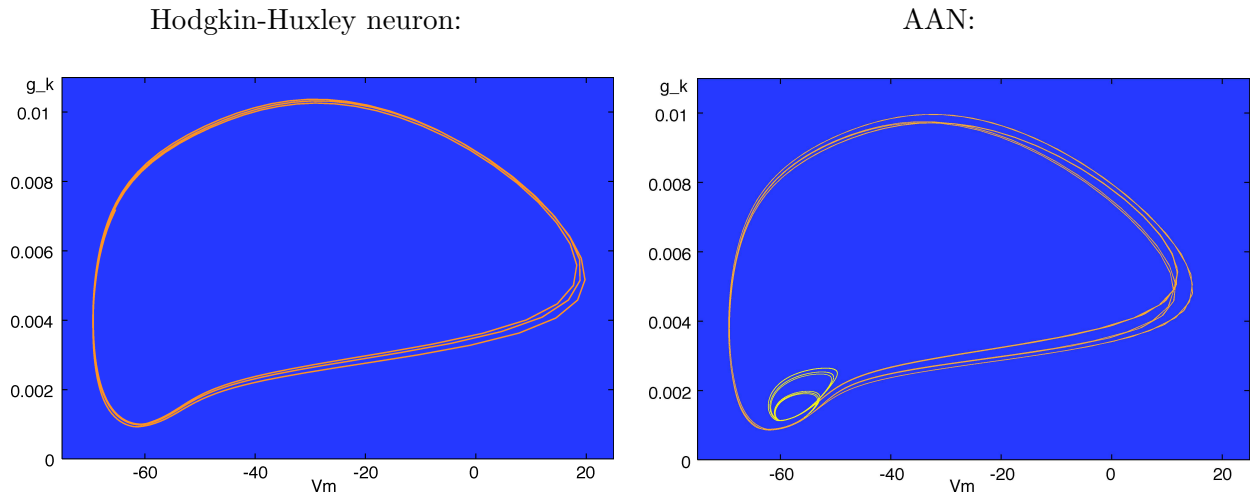


Fig. 7. The conductivity  $g_K$  as a function of the membrane voltage  $V_m$  for the modeled Hodgkin–Huxley neuron without autapse (left) and with autapse (right). The autapse results in a bistable oscillatory behavior.

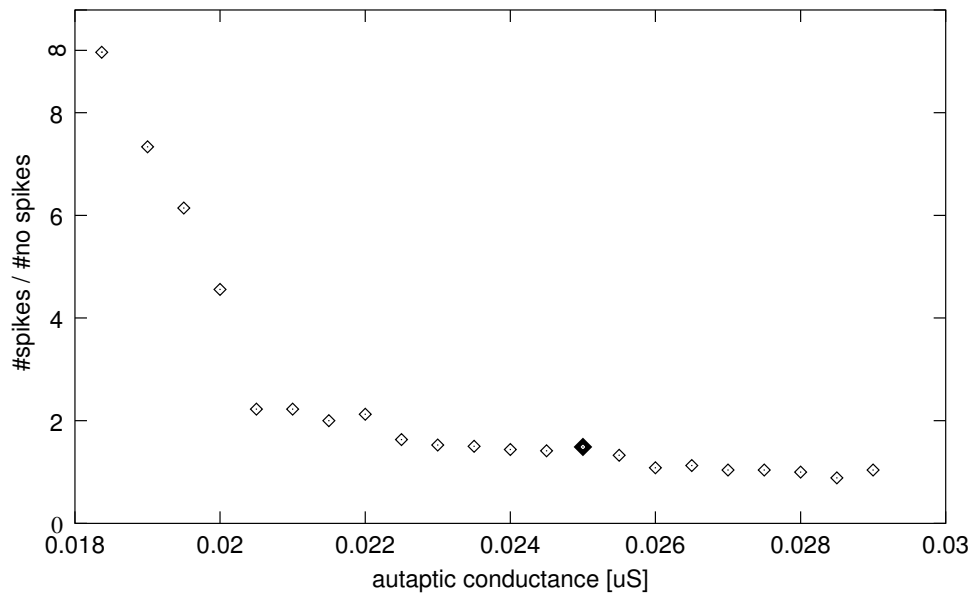


Fig. 8. Ratio of fired action potentials to suppressed action potentials as a function of autaptic conductivity. At zero conductivity (no autapse) the neuron fires continuously without suppressed action potentials. Increasing the strength of the autapse decreases the ratio and leads to the observed pattern of alternating spikes and suppressed spikes. The solid diamond represents the 40 Hz burst mode.

trajectory runs on a circular path which represents the generation of action potentials. The autapse changes this behavior and adds a second circular path which represents the suppressed action potentials where the dendritic input did not exceed the threshold.

In order to investigate the dynamic transition from a model neuron without an autapse to one with an autapse we varied the conductivity

$G_{\text{aut-max}}$  of the autapse and plotted the ratio of fired action potentials to suppressed action potentials in Fig. 8. For no autaptic inhibition (zero conductivity) this ratio would be infinity and it slowly decreases to about 1 for higher conductivities.

Figure 9 displays the firing pattern of the autapse as a function of the autaptic conductivity. For the given time delay of  $\tau_{\text{aut}1} = 4.2$  ms the neuron fires in 40 Hz bursts only at an autaptic

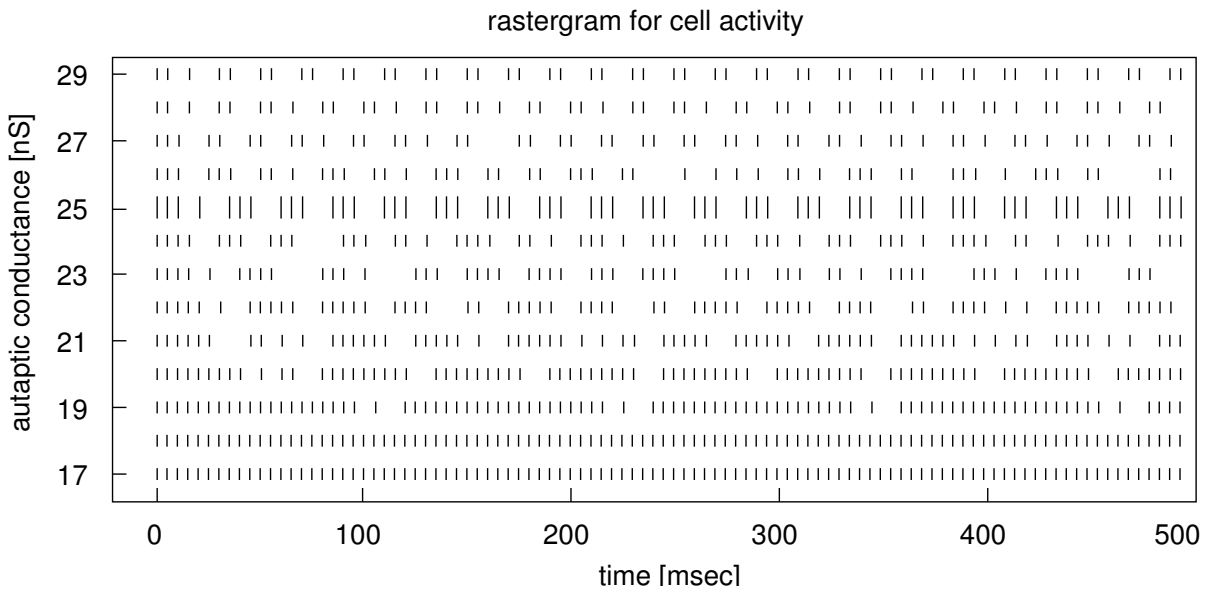


Fig. 9. The rastergram plots the spike trains over time (X-axis) as a function of autaptic conductivity (Y-axis). At low conductivity (no autapse) the neuron fires continuously. At high conductivity the neuron alternates between firing action potentials and suppressing them. At 25 nS the neuron fires in bursts of 40 Hz.

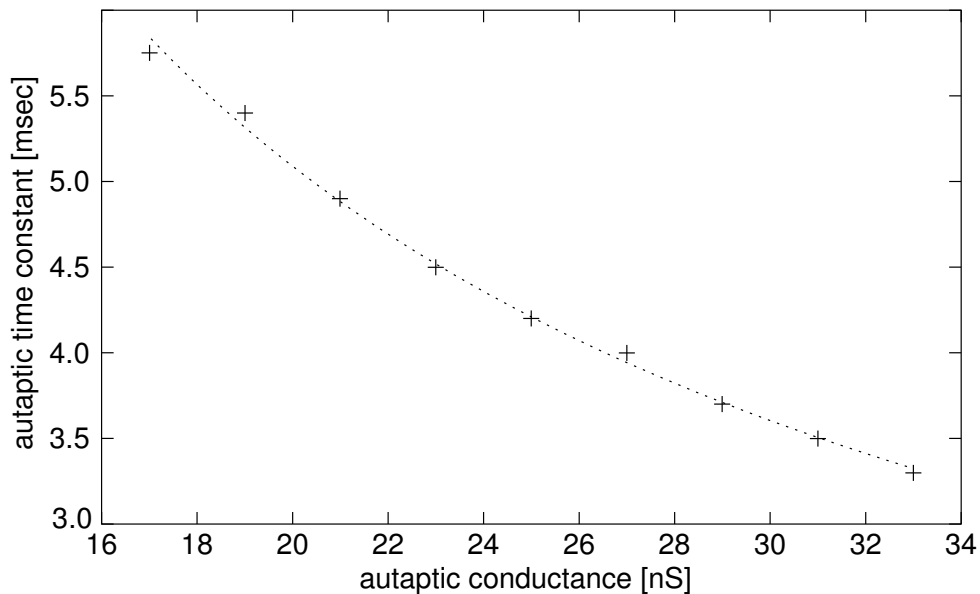


Fig. 10. Correct autaptic time constant  $\tau_{\text{aut}1}$  (Y-axis) as a function of autaptic conductivity  $G_{\text{aut-max}}$  (X-axis) in order to make the neuron fire at bursts of 40 Hz.

conductivity of 25 nS. At 29 nS conductivity another rhythmic firing at 52 Hz is observed. By choosing the right parameters for conductivity and time delay the neuron can always be forced to fire in bursts of 40 Hz. The correct parameter pairs for this behavior are illustrated in Fig. 10.

#### 4. Discussion

Our results demonstrate a potential mechanism of the recently found autapses on neurons. We simulated a realistic model of an inhibitory hippocampal basket cell via the Hodgkin–Huxley equations. As in reality, this cell fires regular action potentials when

driven by sufficient trains of action potentials when no autapse is present. However, when the GABAergic action potential are fed back onto the soma of the cell by an autapse, it fires in spike bursts. This behavior results from the inhibitory autaptic feedback which suppresses a few excitatory postsynaptic potentials (EPSPs). When the firing of the cell has ceased, the autaptic feedback also decreases and the cell can integrate dendritic input again.

The time constant of the synapse,  $\tau_{\text{syn}}$ , and that of the autapse,  $\tau_{\text{aut}}$ , turned out to be critical parameters for our model. If these parameters were varied too much from the values given in Sec. 5, the bursting behavior of the AAN changed to a less orderly state. Also the resting-potential of the neuron was a critical value. As discussed by Shepherd [1998, p. 71], burst firing requires resting-potentials around  $-65$  mV whereas single spike firing is more probable at resting-potentials around  $-55$  mV.

Such oscillators have a number of features which are found in the network which constitutes our brains. For example, if parts of the neural network in our brain consists of neural oscillators which are tuned to specific frequencies then these frequencies should occur more often than others. Such resonance frequencies can indeed be recorded in human electroencephalogram [Herrmann, 2001; Neuper & Pfurtscheller, 2001]. Our results demonstrate that physiologically plausible values for the critical parameters of the AAN yield oscillations with a burst frequency of approximately 40 Hz (with a 200 Hz spike rate within each burst). This frequency is commonly recorded in various physiological and psychological experiments and is assumed to be related to cognitive functions [Engel *et al.*, 2001; Keil *et al.*, 2001].

We are, of course, aware of the fact that the described bursting behavior of the neuron can be achieved by different mechanisms also. Some neurons fire in intrinsic spike bursts [Stanford *et al.*, 1998] and others may be inhibited in a way similar to the autaptic inhibition via interneurons [Traub *et al.*, 1997]. However, our results demonstrate that autapses may also lead to oscillatory behavior in otherwise nonoscillating neurons and offer a potential explanation what their functional role might be.

## 5. Technical Details

The actual model used in our approach is a modification of the model by Wang and Buzsaki [1996].

The capacity of the membrane was chosen to be

$$C_m = 1 \mu\text{F}/\text{cm}^2 \quad (5)$$

The equilibrium potentials for the  $\text{K}^+$  and  $\text{Na}^+$  channels are

$$E_{\text{K}} = -80 \text{ mV} \quad (6)$$

$$E_{\text{Na}} = 55 \text{ mV} \quad (7)$$

To obtain a resting potential of  $-60$  mV the equilibrium voltage of the leakage channels was chosen to be

$$E_L = -50 \text{ mV} \quad (8)$$

Generally, in artificial neurons the resistors are represented by their conductivity  $G$ :

$$G_{\text{Na}} = G_{\text{Na-max}} m^3 h \quad (9)$$

$$G_{\text{K}} = G_{\text{K-max}} n^4 \quad (10)$$

$$G_L = 0.003 \text{ S}/\text{cm}^2 \quad (11)$$

$$G_{\text{Na-max}} = 0.14 \text{ S}/\text{cm}^2 \quad (12)$$

$$G_{\text{K-max}} = 0.036 \text{ S}/\text{cm}^2 \quad (13)$$

The temporal behavior of the ion channels is modeled by two values  $\alpha$  and  $\beta$  where  $\alpha$  determines the rate of ion-transfer into the neuron and  $\beta$  in opposite direction.

$$\frac{dh}{dt} = 4.5 (\alpha_h (1 - h) - \beta_h h) \quad (14)$$

$$\frac{dm}{dt} = 4.5 (\alpha_m (1 - m) - \beta_m m) \quad (15)$$

$$\frac{dn}{dt} = 4.5 (\alpha_n (1 - n) - \beta_n n) \quad (16)$$

The parameters  $h$ ,  $m$  and  $n$  specify the proportion of ions outside the neuron, while  $(1 - h)$ ,  $(1 - m)$  and  $(1 - n)$  specify the proportion of ions inside the neuron [Hodgkin & Huxley, 1952]. They can also be viewed as the probability at which an ion is likely to travel through an ion-channel into the corresponding direction [Dayan & Abbott, 2001, p. 169].

$$\alpha_m = -0.1 \frac{V_m + 38}{e^{\frac{V_m + 38}{-10}} - 1} \quad (17)$$

$$\alpha_h = 0.07 e^{\frac{V_m + 61.5}{-20}} \quad (18)$$

$$\alpha_n = -0.0075 \frac{V_m + 65}{e^{\frac{V_m + 65}{-10}} - 1} \quad (19)$$

$$\beta_m = 4 e^{\frac{V_m + 63}{-18}} \quad (20)$$

$$\beta_h = \frac{1}{e^{\frac{V_m+31.5}{-10}} + 1} \quad (21)$$

$$\beta_n = 0.125e^{\frac{V_m+44}{-200}} \quad (22)$$

The autapse was modeled by an inhibitory ion channel gated by gamma amino butyric acid (GABA). The maximum conductivity of the GABA autapse was set to  $G_{\text{aut-max}} = 0.025 \mu\text{S}$  [Traub & Miles, 1991, p. 51]. The time constants of the autapse were set to  $\tau_{\text{aut1}} = 4.2 \text{ ms}$  and  $\tau_{\text{aut2}} = 0.1 \text{ ms}$  to represent a GABA<sub>A</sub>-gated Cl<sup>-</sup> channel [Traub & Miles, 1991, p. 86]. The equilibrium potential of the autapse was set to  $-80 \text{ mV}$ . The abovementioned normalization factor is calculated according to

$$\varphi_{\text{aut}} = \left( \left( \frac{\tau_{\text{aut2}}}{\tau_{\text{aut1}}} \right)^{\tau_{\text{rise}}/\tau_{\text{aut1}}} - \left( \frac{\tau_{\text{aut2}}}{\tau_{\text{aut1}}} \right)^{\tau_{\text{rise}}/\tau_{\text{aut2}}} \right)^{-1} \quad (23)$$

$$\tau_{\text{rise}} = \frac{\tau_{\text{aut1}}\tau_{\text{aut2}}}{\tau_{\text{aut1}} - \tau_{\text{aut2}}} \quad (24)$$

Our model neuron had six dendrites each with a length of  $200 \mu\text{m}$  and a diameter of  $1.5 \mu\text{m}$ . The diameter of the soma was  $30 \mu\text{m}$  and the axon was  $500 \mu\text{m}$  long and  $6 \mu\text{m}$  thick. The dendritic input had a frequency of  $200 \text{ Hz}$ . The conductivity of synapses was  $0.0055 \mu\text{S}$  per dendrite (i.e.  $0.033 \mu\text{S}$  for all six dendrites). The time constants were  $\tau_{\text{syn1}} = 3 \text{ ms}$  and  $\tau_{\text{syn2}} = 0.1 \text{ ms}$ .  $\varphi_{\text{syn}}$  can be computed just like  $\varphi_{\text{aut}}$  by replacing aut by syn in Eq. (23). The resting-potential of the basket cell was set to  $-60 \text{ mV}$  [Shepherd, 1998, p. 51].

## Acknowledgments

We express our thanks to Andrea Gast-Sandmann and Stephan Liebig for designing the artwork and to Markus Bauer and Elena Skalozub who have worked on student projects contributing to the present results.

## References

- Başar-Eroglu, C., Strüber, D., Schürmann, M., Stadler, M. & Başar, E. [1996] "Gamma-band responses in the brain: A short review of psychophysiological correlates and functional significance," *Int. J. Psychophysiol.* **24**, 101–112.
- Bekkers, J. M. & Stevens, C. F. [1991] "Excitatory and inhibitory autaptic currents in isolated hippocampal neurons maintained in cell culture," *Proc. Natl. Acad. Sci. USA* **88**, 7834–7838.
- Cajal, S. R. Y. [1911] *Histologie du Système Nerveux de l'homme et des Vertébrés* (Maloine Paris).
- Cobb, S. R., Buhl, E. H., Halasy, K., Paulsen, O. & Somogyi, P. [1995] "Synchronization of neuronal activity in hippocampus by individual gabaergic interneurons," *Nature* **378**, 75–78.
- Dayan, P. & Abbott, L. F. [2001] *Theoretical Neuroscience: Computational and Mathematical Modeling of Neural Systems* (MIT Press, Cambridge).
- Eckhorn, R., Dicke, P., Kruse, W. & Reitböck, H. J. [1990] "Stimulus-related facilitation and synchronization among visual cortical areas: Experiments and models," *Nonlinear Dynamics and Neural Networks*, eds. Schuster, H. W. & Singer, W. (VCH), pp. 57–75.
- Engel, A. K., Fries, P. & Singer, W. [2001] "Dynamic predictions: Oscillations and synchrony in top-down processing," *Nature Rev. Neurosci.* **2**, 704–716.
- Freeman, W. J. [2000] *Neurodynamics: An Exploration in Mesoscopic Brain Dynamics* (Springer London).
- Gloor, P. [1998] *The Temporal Lobe and Limbic System* (Oxford University Press, NY).
- Gray, C. M., König, P., Engel, A. K. & Singer, W. [1989] "Oscillatory response in the cat visual cortex exhibit intercolumnar synchronization which reflects global stimulus properties," *Nature* **338**, 334–337.
- Gray, C. M. & McCormick, D. A. [1996] "Chattering cells: Superficial pyramidal neurons contributing to the generation of synchronous oscillations in the visual cortex," *Science* **274**, 109–113.
- Gutnick, M. J. (ed.) [1995] *The Cortical Neuron* (Oxford University Press, NY).
- Haken, H. [1996] *Principles of Brain Functioning* (Springer, Berlin).
- Herrmann, C. S. & Mecklinger, A. [2000] "Magnetoencephalographic responses to illusory figures: Early evoked gamma is affected by processing of stimulus features," *Int. J. Psychophysiol.* **38**, 265–281.
- Herrmann, C. S. [2001] "Human EEG responses to 1–100 Hz flicker: Resonance phenomena in visual cortex and their potential correlation to cognitive phenomena," *Exp. Brain Res.* **137**, 345–353.
- Hines, M. & Carnevale, N. T. [1995] "Computer modeling methods for neurons," *The Handbook of Brain Theory and Neural Networks*, ed. Arbib, M. A. (MIT Press, Cambridge), pp. 226–230.
- Hines, M. L. & Carnevale, N. T. [1997] "The NEURON simulation environment," *Neural Comput.* **9**, 1179–1209.
- Hines, M. L. & Carnevale, N. T. [2001] "NEURON: A tool for neuroscientists," *The Neuroscientist* **7**, 123–135.
- Hodgkin, A. & Huxley, A. [1952] "A quantitative description of membrane current and its application to conduction and excitation in nerve," *J. Physiol.* **117**, 500–544.
- Jefferys, J. G. R., Traub, R. D. & Whittington, M.

- A. [1996] "Neuronal networks for induced 40 Hz rhythms," *Trends Neurosci.* **19**, 202–208.
- Kandel, E. R., Schwartz, J. H. & Jessell, T. M. (eds.) [2000] *Principles of Neural Science* (McGraw-Hill).
- Keil, A., Gruber, T. & Müller, M. M. [2001] "Functional correlates of macroscopic high-frequency brain activity in the human visual system," *Neurosci. Biobehav. Rev.* **25**, 527–534.
- Lübke, J., Markram, H., Frotscher, M. & Sakmann, B. [1996] "Frequency and dendritic distribution of autapses established by layer 5 pyramidal neurons in the developing rat neocortex: Comparison with synaptic innervation of adjacent neurons of the same class," *J. Neuro.* **16**, 3209–3216.
- McCulloch, W. & Pitts, W. [1943] "A logical calculus of the ideas immanent in nervous activity," *Bull. Math. Biophys.* **5**, 115–133.
- Neuper, C. & Pfurtscheller, G. [2001] "Evidence for distinct beta resonance frequencies in human EEG related to specific sensorimotor cortical areas," *Clin. Neurophysiol.* **112**, 2084–2097.
- Rosenzweig, M. R., Breedlove, S. M. & Leiman, A. L. [2001] *Biological Psychology: An Introduction to Behavioral, Cognitive, and Clinical Neuroscience* (Sinauer Associates, Sunderland).
- Rumelhart, D. E. & McClelland, J. L. [1986] *Parallel Distributed Processing: Explorations in the Microstructure of Cognition* (MIT Press, Cambridge).
- Shepherd, G. M. (ed.) [1998] *The Synaptic Organization of the Brain* (Oxford University Press, NY).
- Stanford, I. M., Traub, R. D. & Jefferys, J. G. R. [1998] "Limbic gamma rhythms II. Synaptic and intrinsic mechanisms underlying spike doublets in oscillating subicular neurons," *J. Neurophysiol.* **80**, 162–171.
- Tallon-Baudry, C., Bertrand, O., Delpuech, C. & Pernier, J. [1996] "Stimulus specificity of phase-locked and nonphase-locked 40 Hz visual responses in human," *J. Neurosci.* **16**, 4240–4249.
- Tallon-Baudry, C., Bertrand, O., Wienbruch, C., Ross, B. & Pantev, C. [1997] "Combined EEG and MEG recordings of visual 40 Hz responses to illusory triangles in human," *Neuroreport* **8**, 1103–1107.
- Tamas, G., Buhl, E. & Somogyi, P. [1997] "Massive autaptic self-innervation of gabaergic neurons in cat visual cortex," *J. Neurosci.* **17**, 6352–6364.
- Traub, R. D. & Miles, R. [1991] *Neural Networks of the Hippocampus* (Cambridge University Press, Cambridge).
- Traub, R. D., Jefferys, J. G. R. & Whittington, M. A. [1997] "Simulation of gamma rhythms in networks of interneurons and pyramidal cells," *J. Comput. Neurosci.* **4**, 141–150.
- Wang, X.-J. & Buzsáki, G. [1996] "Gamma oscillations by synaptic inhibition in a hippocampal interneuronal network model," *J. Neurosci.* **16**, 6402–6413.
- Zschocke, S. [1995] *Klinische Elektroenzephalographie* (Springer, Berlin).